Zolala *et al. Journal of Translational Medicine* (2026) 24:252
https://doi.org/10.1186/s12967-026-07734-w

Journal of Translational Medicine

RESEARCH Open Access

Magnetostaltic pumping in an ex vivo extracorporeal membrane oxygenation model

Mohammadreza Zolala[1], Veronique Heim[2], Cécile V. Denis[3,4], Peter J. Lenting[3], Pierre H. Mangin[2] and Thomas M. Hermans[1,5*]

Abstract

Background Extracorporeal membrane oxygenation (ECMO) is a critical rescue therapy for severe respiratory or cardiac failure. However, current blood pumps generate high shear stresses that can damage blood components, leading to hemolysis, loss of von Willebrand factor multimers, and increased risks of bleeding, thrombosis, and organ injury.

Methods We developed novel magnetostaltic pumps that use magnetic liquid interfaces instead of solid walls to transport blood, aiming to reduce mechanical stress on blood cells. Four magnetostaltic pump designs were tested in ex vivo ECMO circuits using human donor blood at clinically relevant flow rates and compared with standard centrifugal and peristaltic pumps.

Results Across all flow rates, magnetostaltic pumps produced less hemolysis than conventional pumps. Under pediatric flow conditions (1 L/min for 48 h), the large-scale magnetostaltic pump (**QR3**) reduced hemolysis by approximately one-third compared with commercial centrifugal pumps and preserved high-molecular-weight von Willebrand factor multimers. Platelet function was unaffected. Small amounts of nanoparticle leakage from the magnetic fluid were detected but remained well below toxic thresholds.

Conclusions Magnetostaltic pumping offers a promising alternative to current ECMO pumps by reducing blood damage. These results support further testing in animal models to evaluate the potential for clinical translation.

Keywords ECMO, Centrifugal pump, Peristaltic pump, Ex vivo model

Background

Extracorporeal membrane oxygenation (ECMO) procedures have surged in recent years to help patients with COVID-19-associated acute respiratory distress syndrome (ARDS) that deteriorate beyond other therapies and ventilation [1–3]. Fortunately, ECMO-capacity had significantly increased in the past decade across centers world-wide to provide patients with this life-support option [4]. Though ECMO mortality has decreased in the previous 50 years [5], it is still significant at 46% overall (ELSO registry, Oct. 2023 report over 2022) [6]. One key issue in ECMO is technical-induced hemolysis—the breaking of red blood cells (RBCs) due to

*Correspondence:
Thomas M. Hermans
Thomas.Hermans@imdea.org
[1]Université de Strasbourg, UMR7140, Strasbourg, France
[2]INSERM, EFS Grand-Est, BPPS UMR-S1255, FMTS, Strasbourg, France
[3]Université Paris-Saclay, INSERM, Hémostase Inflammation Thrombose HITh U1176, Le Kremlin-Bicêtre 94276, France
[4]Centre Hospitalier Régional Universitaire de Nancy, Nancy 54000, France
[5]IMDEA Nanociencia, C/ Faraday 9, Madrid 28049, Spain

high-shear—which can be pump-related (i.e., pump rotational speed, cavitation, venous pressure) [7, 8], or circuit-related—in the oxygenator (by squeezing [9] RBCs) or cannulae. Hemolysis increases plasma free hemoglobin (PFH) in the blood, which is cytotoxic and leads to vasoconstriction (due to NO scavenging), endothelial disfunction and platelet activation/aggregation [10]. This results eventually in renal or even multi-organ failure and increased mortality [10]. In addition, high shear results in loss of high molecular weight von Willebrand Factor (VWF) multimers [11, 12], associated with bleeding [13].

Controversy remains over which type of pump—centrifugal or roller—is the better for ECMO, though centrifugal pumps are most used in practice [14–18]. First generation centrifugal pumps contained a metal shaft, which was a source of pump-head thrombosis [19]. Newer versions have either a low-friction one-point bearing (e.g., Getinge—Rotaflow RF-32) or no bearing at all (e.g., Abbott/Levitronix—CentriMag or Eurofins—Colibri/ECMOLife, fully magnetically levitated) avoiding the latter issue. In addition, second generation centrifugal pump-heads have much reduced priming volumes, no stagnant blood zones, and reduced hemolysis [20, 21]. In terms of bleeding complications, roller pumps show predominant bleeding in the surgical/cannulation sites, whereas centrifugal pumping leads to increased non-surgical bleeding (i.e., neurological, pulmonary, gastrointestinal) [22]. All current pumps have moving solid parts in contact with blood, which inevitably lead to mechanical forces and thus damage to blood components to some extent.

Here we develop a series of magnetostaltic pumps that lack solid walls inside the pump-head and analyze them in ex vivo ECMO model circuits with (and without) membrane oxygenator using human donor blood. Magnetostaltic pumps use a biocompatible magnetic ferrofluid and moving permanent magnets to create a liquid-in-liquid pumping action without having blood contact with any solid surface inside the pump-head. Four different pumps are tested at flow rates 4, 150, or 1000 mL min^{-1} (the latter corresponding to pediatric ECMO conditions), PFH values are measured up to 48 h and additionally at 1000 mL min^{-1} VWF multimers are analyzed. In comparison with centrifugal (**Rotaflow** RFD 20–973 with RF-32 disposable pump head & **Levitronix** PuraLev iF30SU) and peristaltic pumps (**P1**: Lead Fluid BT80S & **P2**: Lead Fluid BT100S) the magnetostaltic pumps have lower PFH as well as reduced loss of high molecular weight VWF multimers. With further development and regulatory approval, magnetostaltic pumping could find applications in ECMO in the future.

Results

We have recently developed a new fluidic paradigm, where any diamagnetic liquid (e.g., blood, water, honey) can flow in channels that have walls consisting of a magnetic ferrofluid [23–26]. Using typically four permanent NdFeB magnets, we can make magnetic fields where the field strength is high, close to the wall, and zero at the center of a channel (called a quadrupole). Upon introducing the ferrofluid—mineral oil with magnetite nanoparticles ~ 10 nm in diameter stabilized by oleic acid surfactants (note: each of the individual components, but not the formulation or its use, is currently FDA approved)—a cavity is formed around the zero magnetic field zone where the diamagnetic liquid can flow. In a previous study, we used curved arc magnets on a static housing, and rotated an impeller also containing arc magnets to achieve a peristaltic-like pumping action we named "magnetostaltic pumping" [23]. This approach was difficult to scale up, because arc magnets in the required sizes are not easily commercially available.

Therefore, we switched to the approach presented here that uses only 1 or 2 cm^3 affordable and available NdFeB (N42 grade) magnets. By positioning 4 magnets in a cross-arrangement with respect to a cylindrical chamber it is possible to create an 'closed' arrangement—allowing only ferrofluid to occupy the space (Fig. 1a), or an 'open' state where blood and ferrofluid are arranged in a concentric arrangement (Fig. 1b). One can see that only 3 magnets need to permeate to switch from open to closed, whereas the top cube magnet remains unchanged (compare top arrow in Fig. 1a to b). A rotary magnetostaltic pump is thus made by having a stator with the magnetization consistently in the downwards orientation (top arrow in Fig. 1a, b), and a rotor containing magnet holders that have alternating open/closed (bottom 3 magnets in Fig. 1a, b) magnet orientations. The rotor moves around a pump chamber that contains a defined amount of ferrofluid, which leads to a pumping action. The pump chamber has a small channel connecting the outlet to the inlet in a high magnetic field region, allowing ferrofluid to travel in a circular motion and not accumulate at the outlet (see Sect. 1 'Chamber optimization' in the Supporting Information). A cross-section of the smallest rotary magnetostaltic pump is shown in Fig. 1d, and Video 1 shows the different pump elements in motion. Three rotary magnetostaltic pumps were made **QR1**, **QR2**, and **QR3** with flow rates up to 14 mL min^{-1}, 200 mL min^{-1} and 1 L min^{-1}, respectively (Fig. 1e–g). **QR1** and **QR2** were 3D printed in black Acrylonitrile Butadiene Styrene (ABS), whereas **QR3** was fabricated using traditional aluminum machining (see methods below). The magnet positioning and geometry of the 3D-printed chamber were optimized to minimize leeching of ferrofluid nanoparticles (see Supporting Information Sect. 1 'Chamber optimization').

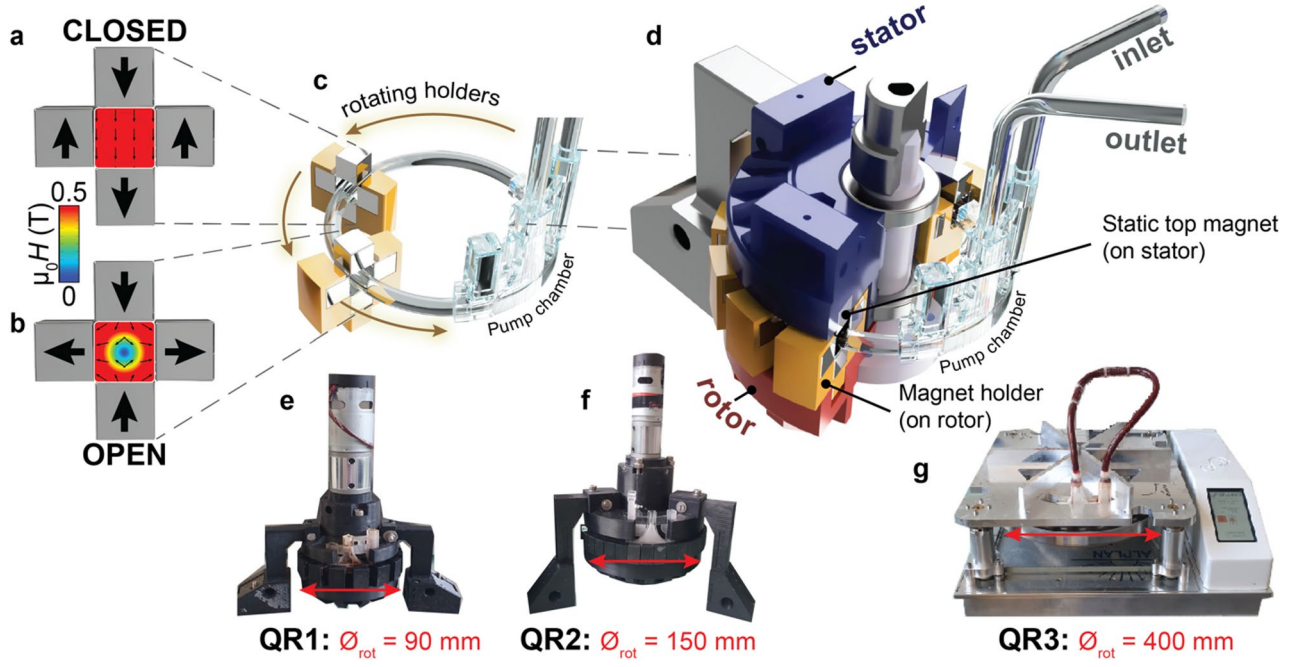

Fig. 1 Rotary magnetostaltic pumps. **a**, "closed configuration": four magnets assembled to yield a high magnetic field (red, 0.5 T), space is fully filled by magnetic ferrofluid. **b**, "open configuration": permutating the 3 bottom magnets leads to a low-field zone at the center (blue–green), which is filled by blood surrounded by ferrofluid. **c**, alternating closed/open magnet holders (holding the bottom 3 magnets in panel **a**, **b**) perform a counter clock-wise rotation around the pump chamber—holding ferrofluid—leading to magnetostaltic pumping. Only two magnet holders are shown for clarity, but there are up to 36 in **QR2** & **QR3**. **d**, cross-sectional view of magnetostaltic pump **QR1** showing: the (blue) stator holding the top magnets of the quadrupoles, (red) rotor holding the (yellow) magnet holders rotating around the pump chamber. See also Supporting Video 1. **e–g**, digital images of pumps **QR1–3** with increasing dimensions and flow rates (see main text)

Having realized that alternating low and high magnetic field regions in motion lead to magnetostaltic pumping, we designed an alternative implementation, resulting in a linear magnetostaltic pump **QL** (Fig. 2). For **QL**, there are 3 rotating shafts (A–C) containing helical arrangements of 1 cm^3 NdFeB magnets, and one static shaft (D) with a linear array of cube magnets. Starting from the open arrangement (Fig. 2a) one can see that clock-wise rotation of shaft A (90°) and B (180°), and counterclockwise for shaft C (−90°) leads to the closed configuration (Fig. 2b). The field at the center of the magnets—where a chamber with ferrofluid is placed (see cross indication)—undergoes changes between high and low magnetic fields (see Video 2 for a front and side view presented side by side). The helical arrangements of magnets along the shafts (except for shaft D)—combined with continuous rotation of the shafts—results in traveling high/low fields from inlet to outlet, leading to linear magnetostaltic pumping. Due to the significant attractive and repulsive forces between the 1 cm^3 cube magnets the shafts were metal-3D-printed, and a gearbox was used to prevent cogging of the electromotor (Fig. 2c). See Video 3 to see the pump in action and the Supporting Information Sect. 2 'Linear pump (**QL**)' for more information. Conveniently, all magnetostaltic pumps (**QR1–3** and **QL**) are self-priming, and do not suffer from burst-failure when the outlet is mechanically blocked (as occurs for peristaltic pumps).

We measured the pump curves for the four pumps (**QR1–3** and **QL**) with water, with the shut-off head increasing from 29 cm H_2O (21.3 mmHg) for **QL** to 135 cm H_2O (99.3 mmHg) for **QR3**. See the best-efficiency-points (BEP) and pressure versus flow rate curves in Supporting Information Sect. 3 'Pump performance curves'. Next, we investigated the use of our new pumps in an ex vivo ECMO model.

ECMO circuit

For pumping at 1000 mL min^{-1} with **QR3**, the Extracorporeal Life Support base tube package (3/8" PVC tubing) was used to connect the pumps and oxygenator (see more details in Supporting Information Sect. 4 'The ECMO circuit'). Air and bubble were removed from the circuit and priming was done using phosphate buffered saline prior to flowing blood (see Sect. 4.2 in the Supporting Information). The blood pH was maintained within 7.35–7.45 and the temperature at 37 ± 1 °C (using a second hot water circuit). The pressure in the circuit was continuously monitored and a pressure-drop check was performed prior to connecting the oxygenator (Quadrox-I by Maquet).

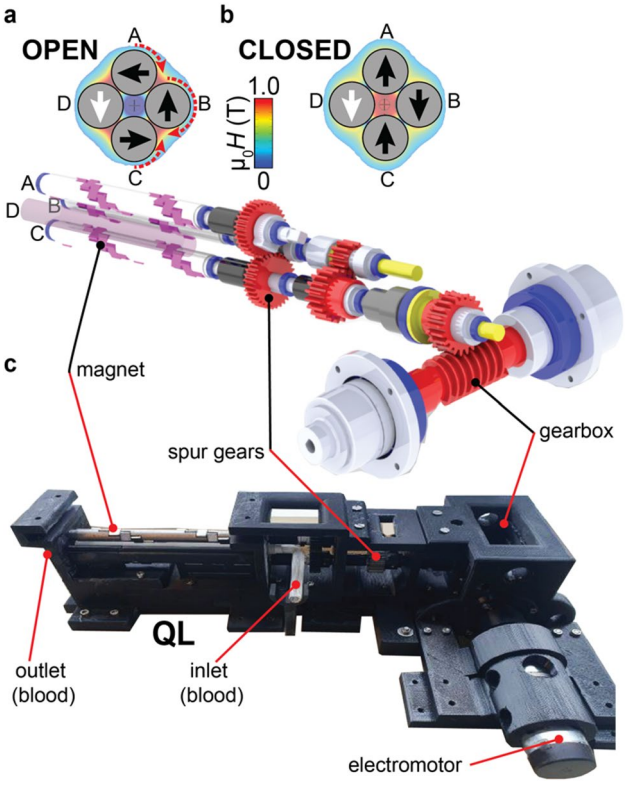

Fig. 2 Linear magnetostaltic pump **QL**. **a**, Magnet arrangement in the "open" configuration. **b**, Arrangement for the "closed" configuration. See Supporting Video 2 for progressions of the low and high magnetic field areas. **c**, Bottom: digital image of **QL** with exposed shafts (see Supporting Information Sect. 2 'Linear pump' for more details). Top: expanded rendered view of the key internal components showing the shafts, magnets, and gearbox

Hemolysis

As mentioned above, our previous study used an arc-magnet Qpump with a maximum flow rate of 1.5 mL min^{-1} (total blood volume 6 mL) for 1 h resulting in PFH values of 12 ± 5 mg dL^{-1}, as compared to a small peristaltic pump where PFH was 130 ± 40 mg dL^{-1} [23]. In the current study, we compare pumps **QR1** (4 mL min^{-1}), **QR2** (150 mL min^{-1}) and **QL** (4 mL min^{-1}) without oxygenator and **QR3** (1000 mL min^{-1}) with oxygenator. The commercial **Rotaflow** and **Levitronix** systems are used only at 1000 mL min^{-1} (corresponding to pediatric cases). We show negative controls—i.e., no pumping, blood was stored statically in a vial—and positive controls with peristaltic pumps (**P1** or **P2**, depending on the flow rate) known to induce high shear.

At the lowest flow of 4 mL min^{-1} the PFH values are very elevated at 101.4 ± 4.5 mg/dL (± standard deviation) even after just 2 h (Fig. 3a) for the peristaltic pump versus 5.5 ± 1.4 mg/dL for the negative control. Both of the smallest magnetostaltic pumps **QR1** and **QL** have significantly lower PFH, but do not significantly differ from each other ('ns' indication in Fig. 3a). At 150 mL min^{-1}, we see a similar picture, where magnetostaltic pumping is significantly less damaging—i.e., lower PFH values—as compared to peristaltic pumping (Fig. 3b). We note that pump **P1** is not designed, nor optimized for blood transport.

Scaling up to 1000 mL min^{-1} we see that the PFH values of **Rotaflow**, **Levitronix** and **QR3** are significantly lower as compared to peristaltic pump **P2** (cf. Figure 3c), but at a limited time of 2 h it is not yet possible to distinguish the former three from each other. This situation changes at longer (48 h) duration experiments, where **QR3** has ~33% lower PFH values as compared to **Rotaflow** and **Levitronix** (see ** indicators in Fig. 3d). In terms of PFH values, **Rotaflow** and **Levitronix** cannot be distinguished under these conditions (see 'ns' in Fig. 3d).

In addition to PFH values, we also assessed the shear damage on VWF multimers for the same samples presented in Fig. 3d. To this end, we first used an ELISA assay [27] that quantifies the ratio of intact (not degraded) VWF to the total amount of VWF (see Sect. 6.3 of the Supporting Information), which shows that both **QR3** as well as **Levitronix** show low (~ 20%) damage. In contrast, **Rotaflow** leads to loss of 58 ± 13% of intact VWF, and **P2** damages 75 ± 7%. The multimers were also analyzed using agarose gel electrophoresis as described in Sect. 6.2 of the Supporting Information, and shown in Fig. 3f, g. The gel band were digitized and normalized as shown in Fig. 3f, which shows that for **P2** only up to 7-mers could be observed, whereas for **Levitronix** and **QR3** up to 13- and 14-mers are present, respectively.

Platelet aggregation studies were also carried out. We did not observe any defect in collagen-, AA- and ADP-induced platelet aggregation when we compared blood before and after 6 h of pumping with the **QR3** pump (see Sect. 7 of the Supporting Information). Indeed, the extent of platelet aggregation was similar regardless of the experimental condition used, indicating that magnetostaltic pumping does not affect the potential of platelet to function (cf. Fig. S18).

Conclusions and discussion

We have shown low-shear magnetostaltic pumping scalable from mL to L min^{-1} in an ex vivo study using human blood, by actuation of affordable and available NdFeB magnets, as a promising alternative to the currently used peristaltic and centrifugal approaches. The mechanism by which magnetostaltic pumping reduces damage of blood components is multifold: (i) inside our pumps we use ferrofluids to actuate blood, thus creating only liquid-liquid contact with a slip-boundary—i.e., the gradient of blood flow velocity and therefore the shear stress and damage are reduced, and (ii) there is no fast moving impeller (with sometimes associated cavitation) in a magnetostaltic pump, which otherwise can cause mechanical

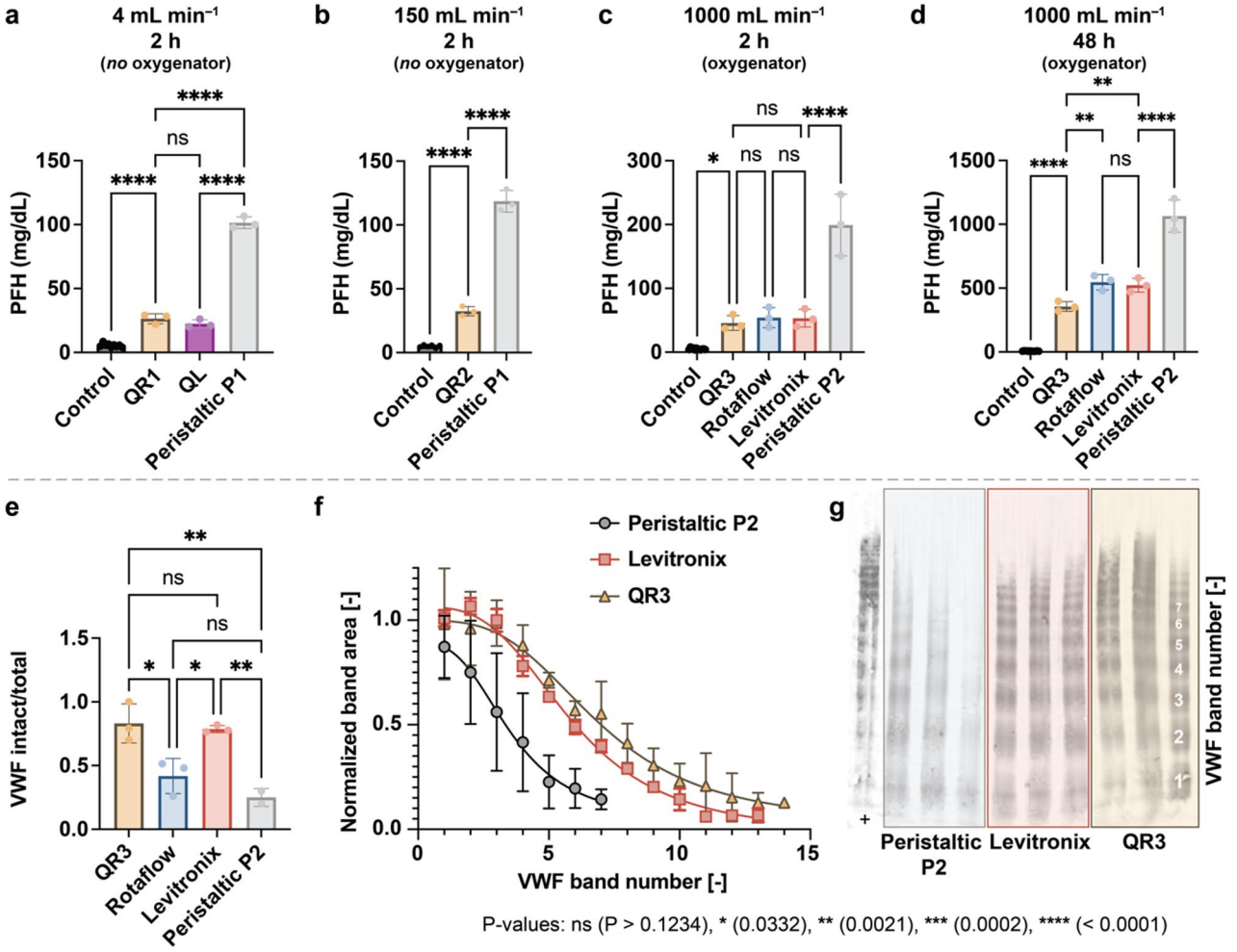

Fig. 3 Comparison of hemolysis and loss of VWF multimers. **a–d**, Hemolysis comparison: plasma free hemoglobin (PFH) for **QR1–3**, **QL** and relevant controls (i.e., "control" = no pumping, and peristaltic **P1** or **P2** comparison). See NIH values of hemolysis in Sect. 4.5 of the Supporting Information. **e–g**, VWF evaluation (after 48 h at 1000 mL min^{-1} pumping with oxygenator): **e**, intact VWF versus total VWF by ELISA testing (see Sect. 6 'Blood analysis' in the Supporting Information). **f**, VWF multimer gel bands (first integrated from panel g and then normalized to 1.0) showing more high molecular weight bands for **QR3**. **g**, digitized gel electrophoresis image, **+** is the DNA ladder for molecular weight determination

impact with blood components. As a result, shear damage is very low for the magnetostaltic pumps—as evidenced by 33% lower PFH values, lower loss of VWF multimers, and negligible impact on platelet (aggregation) function. We expect that further optimization can further reduce shear damage, for example by tuning the viscosity of the used ferrofluid—in previous work we showed that the wall-shear stress depends on the ratio of the flowing medium versus that of the used ferrofluid [24]. A drawback of our approach is the direct contact between a ferrofluid and the transported blood, which results in minor leaching (~ 75 µg L^{-1} of Fe detected for **QR3**, see Sect. 5 of the Supporting Information). In common toxicity studies of magnetite nanoparticles typical concentrations are orders of magnitude higher (~µg/µL) [28], but further safety analysis is surely required. Release of individual nanoparticles from our pumps is unlikely but rather release of micron-sized droplets could occur, possibly leading to issues resembling fat emboli that obstruct pulmonary arterioles and capillaries [29]. Such micro-droplets may also trigger innate immune activation, particularly complement activation–related pseudoallergy (CARPA) [30], driven by hydrophobic interfaces and nanoparticle–protein interactions. Over longer timescales, persistent droplets and magnetite nanoparticles could accumulate in the reticuloendothelial system, where macrophage uptake and incomplete clearance are associated with chronic foreign-body granulomas and low-grade inflammation [31]. In future studies, high-gradient field magnetic separation [32] should be implemented downstream from the pumps, which would likely trap ferrofluid microdroplets and prevent them of reaching a possible animal or patient. In addition, further chamber and magnetic field design (cf. Fig. S4) can likely

reduce or prevent leaching. Regulatory approval of direct blood/ferrofluid contact is not available at this moment, which prevents rapid clinical translation. Currently, a small animal trial is in preparation to provide in vivo validation of our current study, as an important next step. In the longer term, we hope magnetostaltic pumping can be applied to clinical (pediatric) ECMO.

Methods

Sourcing of blood

Human blood was obtained from regular, drug-free, non-smoking donors provided by the Etablissement Français du sang (EFS) in Strasbourg, France. Blood (450 mL) was collected using an anticoagulant containing heparin (30 UI mL^{-1}, Choay, 5000 UI mL^{-1}). Antibiotic solution was added to prevent bacterial contamination [33] (100 mg L^{-1} gentamicin; (Thermo Fisher, 10 mg mL^{-1})). The blood was mixed well with the anticoagulant and used up to 45 min after collection from the donor. As a quality control measure, blood with a free plasma hemoglobin greater than 20 mg dl^{-1} was discarded [34].

Ferrofluid

The ferrofluid was provided by Qfluidics. The ferrofluid is mineral oil-based and the surfactant used is oleic acid. The dynamic viscosities at 25 °C, density and saturation magnetization are 154 mPa s, 1294 kg m^{-3} and 42 mT, respectively. The ferrofluid has a shelf-life of ~ 1 year and is stable in contact with aqueous solution for at least 2 weeks.

Pump construction

See Supporting Information Sects. 1–3.

Blood analysis, VWF gels and ELISA

See Supporting Information Sects. 6–7.

Centrifugal and peristaltic pumps

A Rotaflow pump RFD 20–973 (Maquet, Getinge) consisting of a console, drive and disposable pump heads (RF-32, Getinge) were used. No surface (e.g., heparin) coating was applied to the centrifugal pump. In addition to the Rotaflow pump, the Levitronix PuraLev iF30SU centrifugal pump was also used in the circuit tests. The Levitronix pump heads are disposable product and is made of gamma-stable polypropylene. The peristaltic pumps (BT100S, BT100S and BQ80S, Lead Fluid) served as control methods.

Supplementary Information

The online version contains supplementary material available at https://doi.org/10.1186/s12967-026-07734-w.

Supplementary Material 1: Design and printing of chambers, linear pump manufacturing method, pump performance curves, setup of the ECMO circuit, leaching quantification, blood analysis (incl. VWF quantification), platelets aggregation, and supporting references (PDF). In addition, 3 supporting videos:

Supplementary Material 2: Video S1, design and functioning of rotary pump (MP4)

Supplementary Material 3: Video S2, magnetic simulations of linear pump (MP4)

Supplementary Material 4: Video S3, design and functioning of linear pump (MP4)

Acknowledgements
We thank Lucas Giacchetti and Vincent Marichez for early magnetostaltic pump developments. Eloïse Pascal is acknowledged for expert technical assistance.

Author contributions
MZ, PHM, and TMH designed the study. MZ and TMH designed, developed, and made the magnetostaltic pumps. CVD and PJL provided essential reagents and expertise.

Funding
MZ was funded partially by a PhD fellowship from Région Alsace entitled "Transport de sang à faible cisaillement grâce à une pompe sans parois" and partially by a LabEx CSC grant number ANR-10-LABX-0026_CSC to TMH.

Data availability
The raw data and statistical processing of Fig. 3 can be accessed here: https://github.com/hermanslab/exvivoECMO (prism format).

Declarations

Ethics approval and consent to participate
Not applicable.

Consent for publication
Not applicable.

Competing interests
TMH and MZ have filed patents on the design and use of the rotary and linear magnetostaltic pumps presented in this work. The latter are jointly owned by the University of Strasbourg, EFS, CNRS, INSERM and SATT Conectus Alsace, and licensed to Qfluidics SAS (Illkirch-Graffenstaden, France). Thomas Hermans is a co-founder and shareholder of Qfluidics SAS.

Received: 15 September 2025 / Accepted: 10 January 2026
Published online: 22 January 2026

References

1. Barbaro RP, MacLaren G, Boonstra PS, Combes A, Agerstrand C, Annich G, et al. Extracorporeal membrane oxygenation for COVID-19: evolving outcomes from the international extracorporeal life support organization registry. Lancet. 2021;398(10307):1230–8.
2. MacLaren G. Extracorporeal life support: the ELSO Red Book 6th edition. Extracorporeal Life Support Organization; 2022. 779 p.
3. Tran A, Fernando SM, Rochwerg B, Barbaro RP, Hodgson CL, Munshi L, et al. Prognostic factors associated with mortality among patients receiving veno-venous extracorporeal membrane oxygenation for COVID-19: a systematic review and meta-analysis. Lancet Respiratory Med. 2023;11(3):235–44.
4. Ramanathan K, Antognini D, Combes A, Paden M, Zakhary B, Ogino M, et al. Planning and provision of ECMO services for severe ARDS during the COVID-19 pandemic and other outbreaks of emerging infectious diseases. Lancet Respiratory Med. 2020;8(5):518–26.
5. Bartlett R, Arachichilage DJ, Chitlur M, Hui SKR, Neunert C, Doyle A et al. The history of extracorporeal membrane oxygenation and the development of extracorporeal membrane oxygenation anticoagulation. Semin Thromb

Hemost [Internet]. 2023 Feb 7 [cited 2023 Nov 4]; Available from: http://www.thieme-connect.de/DOI/DOI?10.1055/s-0043-1761488
6. ELSO registry [Internet]. [cited 2023 Nov 4]. Available from: https://www.elso.org/registry
7. Dalton H, Cashen K, Reeder R, Berg R, Shanley T, Newth C, et al. Hemolysis during pediatric extracorporeal membrane oxygenation: associations with Circuitry, Complications, and mortality. Pediatr Crit Care Med. 2018;19(11):1067–76.
8. Allen S, Holena D, Mccunn M, Kohl B, Sarani B. A review of the fundamental principles and evidence base in the use of extracorporeal membrane oxygenation (ECMO) in critically ill adult patients. J Intensive Care Med. 2011;26(1):13–26.
9. Pan Y, Li Y, Li Y, Li J, Chen H. Fatigue of red blood cells under periodic squeezes in ECMO. Proc Natl Acad Sci. 2022;119(49):e2210819119.
10. Lehle K, Philipp A, Zeman F, Lunz D, Lubnow M, Wendel HP, et al. Technical-Induced hemolysis in patients with respiratory failure supported with Veno-Venous ECMO – Prevalence and risk factors. PLoS ONE. 2015;10(11):e0143527.
11. Mazzeffi M, Meyer M, Deatrick K, Taylor B, Kon Z, Herr D, et al. Von Willebrand Factor-GP1ba interactions in venoarterial extracorporeal membrane oxygenation patients. J Cardiothorac Vasc Anesth. 2019;33(8):2125–32.
12. Chan CHH, Simmonds MJ, Fraser KH, Igarashi K, Ki KK, Murashige T, et al. Discrete responses of erythrocytes, platelets, and von Willebrand factor to shear. J Biomech. 2022;130:110898.
13. Chapman K, Seldon M, Richards R, Thrombotic Microangiopathies. Thrombotic thrombocytopenic Purpura, and ADAMTS-13. Semin Thromb Hemost. 2012;38(1):47–54.
14. Sievert AN, Shackelford AG, McCall MM. Trends and emerging technologies in extracorporeal life support: results of the 2006 ECLS survey. J Extra Corpor Technol. 2009 June;41(2):73–8.
15. MacLaren G, Combes A, Bartlett RH. Contemporary extracorporeal membrane oxygenation for adult respiratory failure: life support in the new era. Intensive Care Med. 2012;38(2):210–20.
16. Johnson KN, Carr B, Mychaliska GB, Hirschl RB, Gadepalli SK. Switching to centrifugal pumps May decrease hemolysis rates among pediatric ECMO patients. Perfusion. 2022;37(2):123–7.
17. Dalton HJ, Hoskote A. There and back again: roller pumps versus centrifugal technology in infants on extracorporeal membrane Oxygenation*. Pediatr Crit Care Med. 2019;20(12):1195.
18. O'Halloran CP, Thiagarajan RR, Yarlagadda VV, Barbaro RP, Nasr VG, Rycus P, et al. Outcomes of infants supported with extracorporeal membrane oxygenation using centrifugal versus roller pumps: an analysis from the ELSO registry. Pediatr Crit Care Med. 2019;20(12):1177–84.
19. Hastings SM, Deshpande SR, Wagoner S, Maher K, Ku DN. Thrombosis in centrifugal pumps: location and composition in clinical and in vitro circuits. Int J Artif Organs. 2016;39(4):200–4.
20. Bottrell S, Bennett M, Augustin S, Thuys C, Schultz B, Horton A et al. A comparison study of haemolysis production in three contemporary centrifugal pumps. Perfusion 2014 Sept 1;29(5):411–6.
21. Ündar A, Wang S, Özyüksel A, Rossano JW. Pediatric devices. In: Mechanical Circulatory and Respiratory Support [Internet]. Elsevier; 2018 [cited 2022 Nov 29]. pp. 271–97. Available from: https://linkinghub.elsevier.com/retrieve/pii/B9780128104910000096
22. Halaweish I, Cole A, Cooley E, Lynch WR, Haft JW. Roller and centrifugal pumps: a retrospective comparison of bleeding complications in extracorporeal membrane oxygenation. ASAIO J. 2015 Sept;61(5):496–501.
23. Dunne P, Adachi T, Dev AA, Sorrenti A, Giacchetti L, Bonnin A, et al. Liquid flow and control without solid walls. Nature. 2020;581(7806):58–62.
24. Dev AA, Dunne P, Hermans TM, Doudin B. Fluid drag reduction by magnetic confinement. Langmuir. 2022;38(2):719–26.
25. Doudin B, Coey M, Cēbers A, editors. Magnetic Microhydrodynamics: An Emerging Research Field [Internet]. Cham: Springer International Publishing; 2024 [cited 2024 Oct 23]. (Topics in Applied Physics; vol. 120). Available from: https://link.springer.com/https://doi.org/10.1007/978-3-031-58376-6
26. Dev AA, Hermans TM, Doudin B. Ultra-soft liquid-ferrofluid interfaces. Adv Funct Mater. 2024 Sept 26;2411811.
27. Kizlik-Masson C, Peyron I, Gangnard S, Le Goff G, Lenoir SM, Damodaran S, et al. A nanobody against the VWF A3 domain detects ADAMTS13-induced proteolysis in congenital and acquired VWD. Blood. 2023;141(12):1457–68.
28. Vazhnichaya E, Semaka O, Lutsenko R, Bobrova N, Kurapov Y. Toxicity factors of magnetite nanoparticles and methods of their research. Innov Biosyst Bioeng. 2024;8(1):3–18.
29. Gossling HR, Pellegrini VDJ. Fat embolism syndrome: A review of the pathophysiology and physiological basis of treatment. Clin Orthop Relat Res. 1982;165:68.
30. Szebeni J. Complement activation-related pseudoallergy: A new class of drug-induced acute immune toxicity. Toxicology. 2005;216(2):106–21.
31. Liu J, Liu Z, Pang Y, Zhou H. The interaction between nanoparticles and immune system: application in the treatment of inflammatory diseases. J Nanobiotechnol. 2022;20(1):127.
32. Moeser GD, Roach KA, Green WH, Alan Hatton T, Laibinis PE. High-gradient magnetic separation of coated magnetic nanoparticles. AIChE J. 2004;50(11):2835–48.
33. Tayama E, Shimono T, Makinouchi K, Ohtsubo S, Nakazawa S, Takami Y et al. Reconsideration of total erythrocyte destruction phenomenon. Artif Organs. 1997;21(7):704–9.
34. Standard practice for assessment of hemolysis in continuous flow blood pumps. In: American Society for Testing and Materials 100 Barr Harbor Dr, West Conshohocken, PA 19428 Reprinted from the Annual Book of ASTM Standards Copyright AST. 1998.

Publisher's note